The motion of a ball moving down a circular path

Diego C. de Souza and Vitor R. Coluci

Citation: American Journal of Physics **85**, 124 (2017); doi: 10.1119/1.4972177
View online: http://dx.doi.org/10.1119/1.4972177
View Table of Contents: http://aapt.scitation.org/toc/ajp/85/2
Published by the American Association of Physics Teachers

The motion of a ball moving down a circular path

Diego C. de Souza and Vitor R. Coluci[a)]
School of Technology, University of Campinas, UNICAMP, Limeira, SP 13484-332, Brazil

(Received 13 April 2016; accepted 30 November 2016)

The problem of a body slipping down a frictionless hemisphere is very common in physics and engineering textbooks. In this type of problem, students are normally asked to find the angle at which the body flies off the surface. In this work, we have constructed an apparatus to determine the angle at which a ball flies off a circular track, and to study the motion of the ball (rolling and slipping) along the surface. The apparatus is comprised of two parallel rails that form a quarter circle. The angular position and velocity of a steel ball are measured using a moveable arm equipped with a photodetector. Two methods are used to determine the angle the ball loses contact with the track. Both methods provide values in agreement with a model for rolling followed by slipping.
[http://dx.doi.org/10.1119/1.4972177]

I. INTRODUCTION

"What height does the boy lose contact with the ice?"[1] This is a typical question of undergraduate physics and engineering textbooks regarding the problem of a body sliding down a frictionless circular path.[1–3] Under these conditions, the height is determined from the angle at which the boy loses contact with the ice, which turns out to be 48.2°, measured from the top of the path. When friction is present, the phenomenon changes, and for a circular object, both slipping and rolling can be present in the motion. A related problem, treated in Symon's seminal book,[4] that has "little practical importance, but which is quite instructive, is that in which one cylinder rolls upon another."

Transforming textbook problems into real experiments provides an interesting way to liven up a physics class by discussing a real situation with students. Besides catching the attention of students, incorporating such experiments in class or laboratory creates an environment prone to discussions regarding apparatus construction, measurement details and difficulties, data analysis, and the comparison between theory and experiment.

In this paper, we describe the construction of an apparatus to determine the angle at which a ball loses contact with a circular track. The apparatus allows students to discuss friction, slipping, and rolling by working with a real experiment inspired from the idealized, textbook physics problem. Whereas, rolling and slipping have been studied by various authors in the last 30 years,[5–12] to our knowledge this is the first work that considers the circular path as discussed in physics textbooks.

In this paper, we first present the model to describe the phenomenon and the methods we have proposed to determine the angle at which the ball loses contact with the track. We then present the details of the apparatus. Finally, we present our results and some discussion about the motion of the ball on the track.

II. THEORETICAL MODEL

A ball of radius r_b and mass m is released from rest at a small ($\ll 1°$) angle θ_0 from the top of a circular track of radius a (Fig. 1). The track consists of two parallel rails whose separation distance is l, which gives the ball an effective radius $r_{\text{eff}} = \alpha a = \sqrt{r_b^2 - (l/2)^2}$ while on the track (our notation parallels that of Ref. 4). Due to friction between the ball and the track, the ball begins its descent by rolling. At an angle θ_s the ball begins slipping, and this slipping continues until the ball reaches an angle θ_c ($>\theta_s$), when the normal force exerted by the track on the ball becomes zero. At θ_c the ball loses contact with the track and freely falls for a time t_f, at which point it lands on the ground a distance d from the point where it would be in contact with the circular track (see Fig. 1).

Because the motion of the ball is constrained by the circular track, we use the Lagrangian formulation to obtain the equations of motion and the relationship between the ball's (translational) velocity and its angular position. The relationship between the velocity and angular position of the ball is used to determine whether the ball is purely rolling or slipping. We follow the procedure used by Symon[4] to describe the motion of one cylinder rolling on another. Using polar coordinates (r, θ) to describe the center of mass of the ball, the Lagrangian $\mathcal{L}$ of the system is written as

$$\begin{aligned}\mathcal{L} &= \frac{1}{2}m\left(\dot{r}^2 + r^2\dot{\theta}^2\right) + \frac{1}{2}I\dot{\varphi}^2 - mgr\cos\theta \\ &= \frac{1}{2}m\left(\dot{r}^2 + r^2\dot{\theta}^2\right) + \frac{1}{2}I\left(\frac{1+\alpha}{\alpha}\right)^2 \\ &\quad \times \left(\dot{\theta}^2 - 2\dot{\theta}\dot{\gamma} + \dot{\gamma}^2\right) - mgr\cos\theta, \end{aligned} \tag{1}$$

where $I = (2/5)mr_b^2$, g is the gravitational field strength, $\gamma \equiv \theta - \alpha\varphi/(1+\alpha)$ is the slip angle, and φ describes the ball's rotation along its axis.

During the pure rolling phase of motion, two constraints are imposed to the ball

$$\begin{aligned} f_1(\theta, \varphi) &= \theta - \left(\frac{\alpha}{1+\alpha}\right)\varphi = 0 \quad \text{and} \\ f_2(r) &= r - (1+\alpha)a = 0. \end{aligned} \tag{2}$$

The first constraint ensures that the ball does not slip ($\gamma = 0$) while the second ensures that the ball remains in contact with the hemisphere. Solving Lagrange's equations subject to these constraints, we obtain a relationship between the angular position θ of the ball's center of mass and its time derivative $\dot{\theta}$ given by

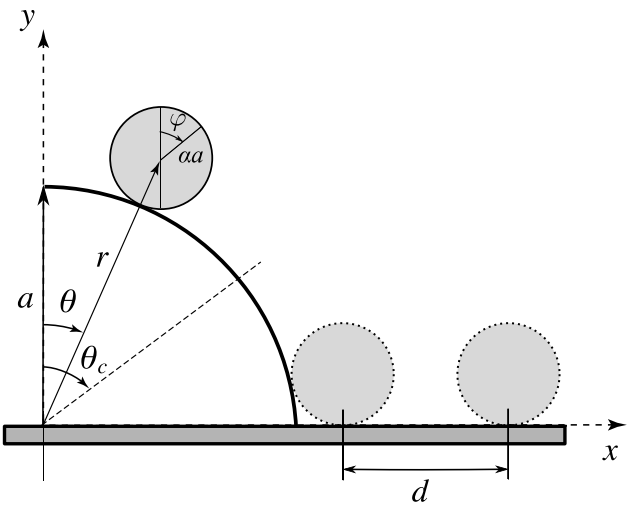

Fig. 1. Schematic of the motion of a ball on a circular path. The position of the ball is given by variable r and θ, whereas the rotation of the ball is quantified by φ. Angle θ_c is where the ball loses contact with the track and starts its free fall. The ball impacts the ground a horizontal distance d from where it would be in contact with the circle.

$$\dot{\theta} = 2\left(\frac{\beta g}{a}\right)^{1/2} \sin\left(\frac{\theta}{2}\right), \tag{3}$$

where $\beta = 5/[(5+2\eta)(1+\alpha)]$ and $\eta \equiv (r_b/\alpha a)^2$.

The forces of constraint, which are the frictional force f and the normal force F exerted by the track on the ball, are found to be $f = 2\eta mg \sin\theta/(5+2\eta)$ and $F = mg[(15+2\eta)\cos\theta - 10]/(5+2\eta)$. As long as the ball rolls without slipping, the condition $f = \mu_s F$ will be satisfied, where μ_s is the coefficient of static friction. Note that μ_s can take on any value between zero and some maximum value μ. Therefore, the maximum angle θ_s that the ball rolls without slipping is obtained from the condition $f = \mu F$, which leads to

$$\cos\theta_s = \frac{(150+20\eta)\mu^2 + 2\eta\sqrt{4\eta^2(1+\mu^2)+60\eta\mu^2+125\mu^2}}{4\eta^2(1+\mu^2)+60\eta\mu^2+225\mu^2}. \tag{4}$$

For $\theta_s < \theta < \theta_c$, the ball begins slipping, so only the constraint $f_2 = 0$ holds. For the simplified case where slipping occurs with no friction, we resolve Lagrange's equations (subject to $f_2 = 0$), which leads to

$$\int_{\dot{\theta}_s}^{\dot{\theta}} \dot{\theta}\, d\dot{\theta} = \int_{\theta_s}^{\theta} \frac{g\sin\theta}{a(1+\alpha)} d\theta, \tag{5}$$

where $\dot{\theta}_s$ is given by Eq. (3) with $\theta = \theta_s$. Integrating Eq. (5) leads to the relation between θ and $\dot{\theta}$, which can then be used to determine the normal reaction force F. Setting $F = 0$ then gives the angle θ_{c0} the ball flies off the track (when there is no friction after slipping occurs) as

$$\cos\theta_{c0} = \frac{2}{15+6\eta}(5+2\eta\cos\theta_s). \tag{6}$$

For a completely frictionless surface, the ball will begin slipping immediately (at a nonzero $\theta \ll 1°$) so that $\cos\theta_s = 1$. Taking $\eta = 1$ (the effective radius of the ball is equal to the actual radius of the ball) then leads to the standard problem of a mass sliding without friction on a spherical surface. In this case, Eq. (6) reduces to $\cos\theta_{c0} = 2/3$, as expected.

To obtain the equation of motion when the ball is slipping on the track in the presence of friction, we need to include Rayleigh's dissipation function[13] $\mathcal{F} = \mu mga(1+\alpha)\dot{\theta}\cos\theta$ in Lagrange's equations.[14] In this case, the relationship between $\dot{\theta}$ and θ becomes

$$\dot{\theta} = 2\left(\frac{\beta' g}{a}\right)^{1/2} \left[\beta(1+\alpha)\sin^2(\theta_s/2) + \frac{1}{2}(\cos\theta_s + \mu\sin\theta_s - \cos\theta - \mu\sin\theta)\right]^{1/2}, \tag{7}$$

where $\beta' \equiv 1/(1+\alpha)$. In this case, the angle the ball loses contact with track (in the presence of friction) is given by

$$\cos\theta_{c\mu} = \frac{2\left[g_1(\eta,\theta_s) - 3\mu\sin\theta_s - \mu\sqrt{g_2(\mu,\alpha,\beta,\theta_s)}\right]}{9+4\mu^2}, \tag{8}$$

where

$$g_1(\eta,\theta_s) \equiv 3\cos\theta_s + 3\beta(1+\alpha)(1-\cos\theta_s), \tag{9}$$

and

$$g_2(\mu,\alpha,\beta,\theta_s) \equiv 9 + 4(\mu^2-1)\cos^2\theta_s - 16\beta(1+\alpha)[\beta(1+\alpha)\sin^2(\theta_s/2) + \mu\sin\theta_s]\sin^2(\theta_s/2) - 8[2\beta(1+\alpha)\sin^2(\theta_s/2) + \mu\sin\theta_s]\cos\theta_s. \tag{10}$$

Figure 2 shows the behavior of the angles θ_s, θ_{c0}, and $\theta_{c\mu}$ as the (maximum) coefficient of static friction μ varies from 0 to 1. As seen in this figure, the variation of θ_s as a function of μ is fairly large, about 45°, whereas θ_{c0} and $\theta_{c\mu}$ exhibit much smaller variations of about 10°.

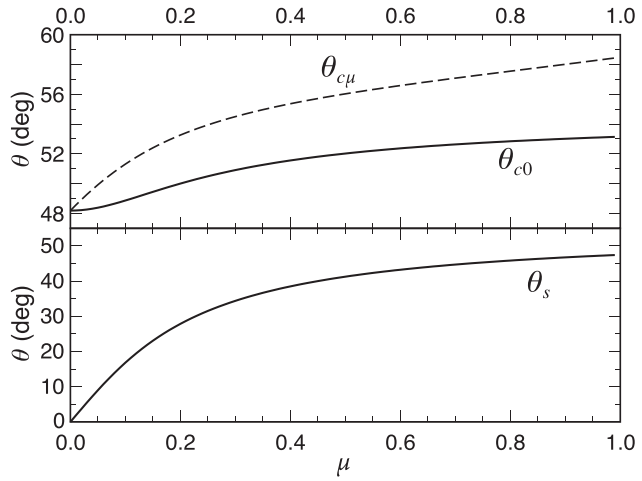

Fig. 2. Behavior of θ_s, θ_{c0}, and $\theta_{c\mu}$ as a function of the coefficient of static friction.

III. MEASURING THE ANGLE THE BALL FLIES OFF THE TRACK

We considered two methods to determine the angle the ball flies off the track. In Method I, the angle θ_c was determined by measuring the time evolution of the angular position of the ball, $\theta(t)$, and determining the exact time t_c the ball loses contact with the rails. We then have $\theta_c = \theta(t_c)$.

In Method II, we use data from when the ball has already flied off the track. The x and y coordinates of the center of mass of the ball during free fall depend on θ_c and on the time of flight t through

$$x(\theta_c, t) = R\sin\theta_c + (v_c\cos\theta_c)t, \tag{11}$$

and

$$y(\theta_c, t) = R\cos\theta_c - (v_c\sin\theta_c)t - \frac{1}{2}gt^2, \tag{12}$$

where $R \equiv a(\alpha+1)$ and v_c is the speed of the center of mass of the ball at the moment it loses contact with the surface. Equations (11) and (12) hold from the moment the ball loses contact with surface until it collides with the table. If the total free-fall flight time is t_f, then at the moment of impact with the table we have $x = R + d$, $y = r_b$, and $t = t_f$ (see Fig. 1). Plugging these values into Eqs. (11) and (12) allows us to solve for θ_c and v_c in terms of the measurable quantities d and t_f. The results are

$$\cos\theta_c = \frac{AB + \sqrt{1 - A^2 + B^2}}{1 + B^2}, \tag{13}$$

and

$$v_c = \frac{d + a(\alpha+1)(1-\sin\theta_c)}{(\cos\theta_c)t_f}, \tag{14}$$

where

$$A \equiv \frac{(\alpha+1)a}{(\alpha+1)a + d}, \tag{15}$$

and

$$B \equiv \frac{r_b + gt_f^2/2}{(\alpha+1)a + d}. \tag{16}$$

Thus, we can determine θ_c by measuring d and t_f and using Eq. (13).

IV. APPARATUS

Two electrically isolated aluminum plates make up the circular track for the steel ball (Fig. 3). A quarter circle track was constructed using computerized machining in order to guarantee a circular path as much as possible. We used the two plates as part of an electronic circuit with the ball acting as a switch between the plates. When the ball is on the track, an electrical contact between the plates is established that produces a `HIGH` signal. When the ball loses contact with at least one of the plates, a `LOW` signal is produced. In this way, we can determine the time t_c at which the ball flies off the track.

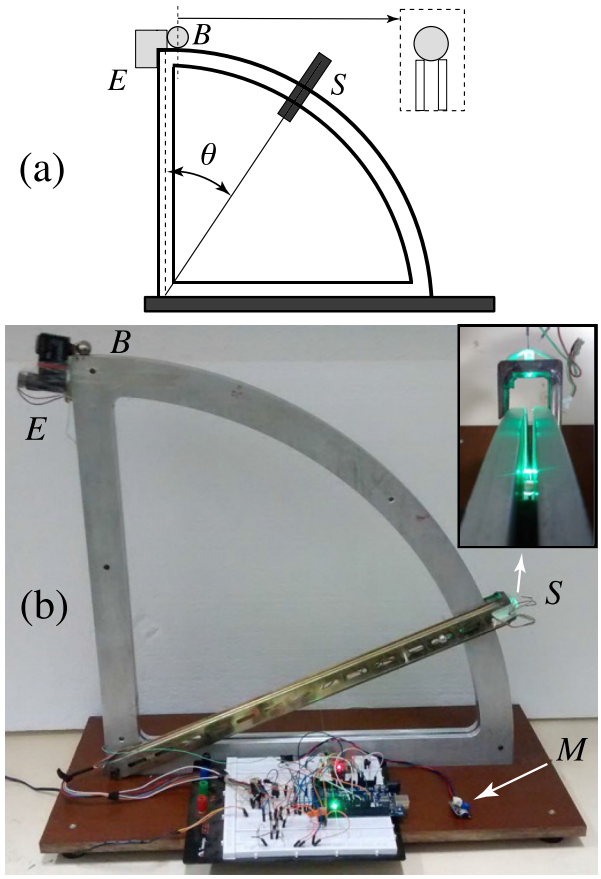

Fig. 3. The apparatus used to determine the angle the ball loses contact with a circular track: (a) schematic diagram and (b) photograph that shows the ball B, the optical detector S, the electromagnetic device E to release the ball, and the microphone M. The inset in (a) shows the separated plates used to keep the ball on the circular path. The inset in (b) shows the optical sensor; the LED is placed below the track with the photodetector above.

An electromagnet—a solenoid extracted from an electrovalve (Microar, 12 V, 4 W, Part No. 0200000113)—is used to release the ball at the top of the track. In addition, the ball is also used as an electrical switch to start the timer. At the top of the track, a small copper plate is placed between the electromagnet and the ball. When the electromagnet is on, the ball stays in contact with the cooper plate. When the ball loses contact with the copper plate (by turning off the electromagnet), the timer is started.

A photodetector, comprised of a green LED and a phototransistor, is placed in a moveable arm. This photodetector is used to measure the angular position θ of the ball on the track, and the ball velocity is determined from the ratio of the ball diameter to the time the ball interrupts the light on the photodetector. These photodetector measurements are used to obtain the angle θ_c at which the ball loses contact with the track. In addition, we also determined θ_c using the total free-fall time t_f and the location d where the ball impacts the ground (see Fig. 1). The free-fall time was found by measuring the sound (using an analog sound sensor, HR 11080 from DFRobot[15]) produced by the ball during its motion on the track and the sound the ball makes upon the impact with the ground, while the impact point was measured using carbon paper to record the ball's impact with the ground.

An Arduino Mega 2560 is used to control the electromagnet, to record data from the photodetector and microphone, and to collect time data from the moment the ball is released

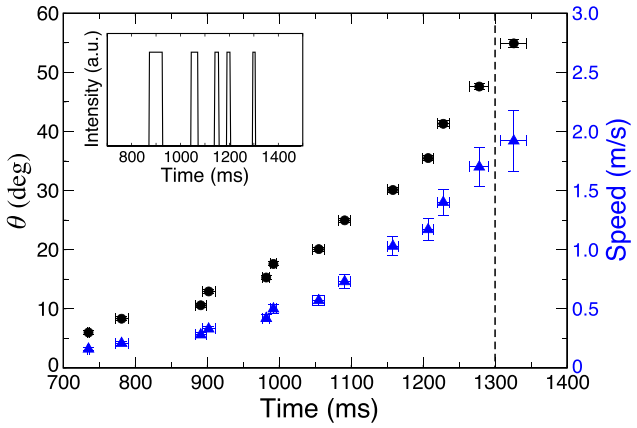

Fig. 4. Time evolution of the angular position of the ball (left) and the (translational) ball speed (right); the dashed line indicates the time the ball flies off the track. The inset shows superimposed photodetector data from five experiments with the arm at different locations.

until it impacts the table; the data were saved using an SD Module (DFR0071 from DFRobot[16]). The Arduino code and the electronic circuits used are available as supplementary material.[17] The Arduino was chosen because it is relatively inexpensive and is accessible in most undergraduate teaching laboratories. To validate data from the Arduino, we have also collected data for some experiments using a Tektronix TBS1052B-EDU 50-MHz digital oscilloscope.

The geometrical characteristics of our apparatus are: $r_b = 7.50 \pm 0.05$ mm, $a = 487 \pm 1$ mm, $\theta_0 = 0.29 \pm 0.12°$, $l = 5.0 \pm 0.5$ mm, and $\eta = 1.12$. The (maximum) coefficient of static friction between the ball and the aluminum plates was $\mu = 0.21 \pm 0.01$. This value was measured by joining two balls together using adhesive tape and placing them on the straight part of the setup (the bottom portion of the track in Fig. 3). The angle with the horizontal was then slowly increased until the pair of balls starts to move (at angle γ, with $\mu = \tan\gamma$). Using the measured μ, the predicted angles from Eqs. (4), (6), and (8) are found to be $\theta_s = 28.7 \pm 0.8°$, $\theta_{c0} = 50.1 \pm 0.1°$, and $\theta_{c\mu} = 53.4 \pm 0.1°$.

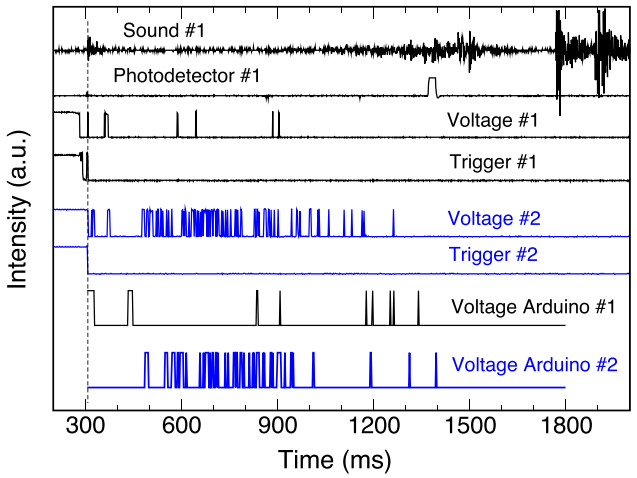

Fig. 5. Typical measurements for sound, photodetection, and voltage between the plates obtained from the oscilloscope and the Arduino (voltage only). Two different experiment results are shown as black and gray (blue online) as voltage #1 and #2. The vertical dashed line indicates the moment used as the time origin when the trigger is turned on.

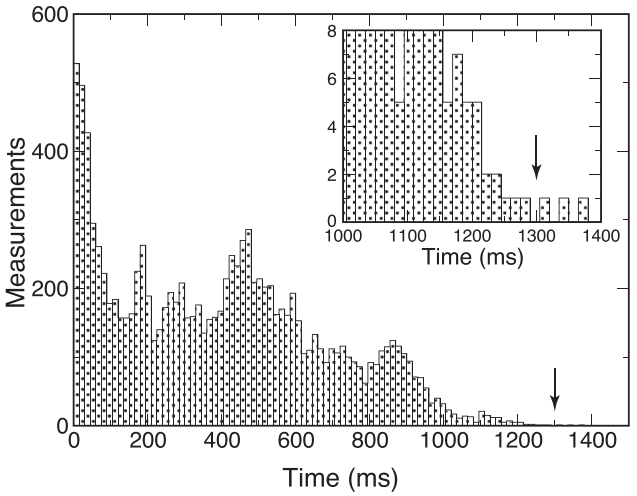

Fig. 6. Histogram of the voltage measurements for 324 runs. The arrow indicates the estimated time (1300 ms) that the ball loses contact with the track (the inset shows a zoomed-in view). For each run, 700 voltage measurements were made during the 1500 ms. The histogram was built using only measurements that indicated the ball was in contact with the rail, which corresponds to 11336 total measurements.

V. EXPERIMENT AND RESULTS

The angular position of the ball and the speed of its center of mass are shown in Fig. 4. Data from the photodetector revealed, as expected, an increase in the ball speed as the ball moves down the track (inset). Whereas, the photodetector data from the Arduino were easily reproducible, measurements of the voltage between the plates exhibited a large variation from independent runs of the experiment (Fig. 5). Measurements from the oscilloscope confirmed this variation. We attribute this behavior to irregularities present on the track that cause the ball to temporarily lose contact with the track and, consequently, change the voltage signal. Therefore, to obtain t_c we repeated the experiment (ball release) over 300 times and created a histogram of the voltage data (Fig. 6). Although we observed voltage signals up

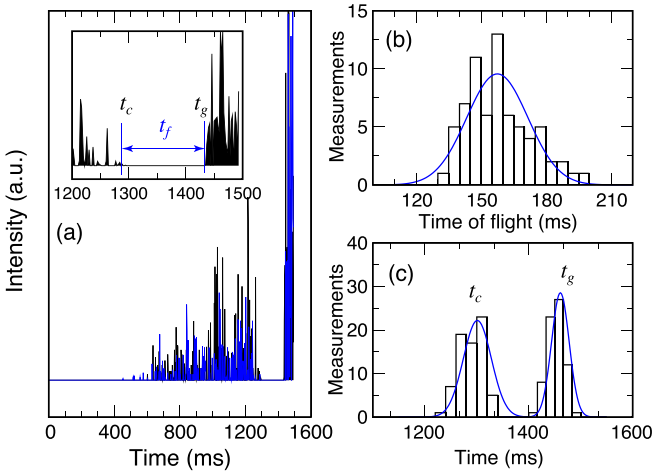

Fig. 7. (a) Time evolution of the sound during the motion of the ball. Data from two different runs of the experiment are shown. The inset graph shows the time the ball flies off the track (t_c), the time the ball hits the ground (t_g), and the free-fall time of flight ($t_f = t_g - t_c$). (b) Histogram for the time of flight (72 runs). (c) Histograms for t_c and t_g. Gaussian fits to the histograms are shown in gray (blue online).

to about 1380 ms, we took the first gap in the measurements to be the time the ball lost contact with the surface (see inset), giving $t_c = 1300 \pm 5$ ms. This value was also confirmed from the sound data (see Fig. 7). Using $t_c = 1300$ ms, we estimated θ_c from Fig. 4 to be $\theta_c = 52 \pm 2°$, which is consistent with the predicted value of 53.4° in the presence of friction with $\mu = 0.21$.

Detectable data for sound from the Arduino started at about 500 ms (Fig. 7). From that time on, we observed an irregular signal pattern up to about 1300 ms. No detectable signal is observed between about 1300 ms and 1450 ms when the ball is in free fall. The abrupt increase of the sound signal at about 1450 ms is due to the impact of the ball with the ground ($y = 0$, Fig. 1). The time the ball flies off the track (t_c), the time the ball reaches the ground (t_g), and the free-fall time of flight (t_f) obtained from the sound data exhibited an approximately gaussian distribution, as shown in Figs. 7(b) and 7(c). The narrow distribution of t_g indicates the good reproducibility presented by the apparatus. From the fitted gaussian curves, we obtain $t_c = 1301 \pm 38$ ms, $t_g = 1460 \pm 24$ ms, and $t_f = 157 \pm 20$ ms. The time the ball flies off the track obtained by the sound measurements is in agreement with the one estimated from the voltage measurements.

Determined from 60 experiments, the location of the impact point of the ball with the ground was $d = 50.5 \pm 0.6$ mm. From the measured values of d and t_f, we obtained $\theta_c = 48 \pm 4°$ and $v_c = 1.65 \pm 0.09$ m/s from Eqs. (13) and (14), respectively. Again, we find a value of θ_c close to the prediction.

The apparatus described here also allows studying the motion of the ball while on the track. An analysis of $\dot{\theta}$ vs $\sin(\theta/2)$ based on Eqs. (3) and (7) provides a way to determine whether the ball is rolling or slipping. Such plots (or similar ones, e.g., involving acceleration) have been used by other authors to study rolling and slipping.[5,6,10] As shown in Fig. 8, we observed two different behaviors. A linear fit of the data for $\sin(\theta/2) < 0.2$ provides a slope of 3.5 ± 0.1 m/s, which is very close to the predicted value of 3.65 m/s for pure rolling given by Eq. (3). For $\sin(\theta/2) > 0.25$, Eq. (7) correctly describes the motion for a friction coefficient close to 0.15. For $\mu = 0.15$, the predicted angles are $\theta_s = 23.1 \pm 0.8°$, $\theta_{c0} = 49.5 \pm 0.1°$, and $\theta_{c\mu} = 52.4 \pm 0.1°$. This friction coefficient is smaller than the measured value of $\mu = 0.21$. This discrepancy might be explained by the fact that we measured the maximum static friction, whereas a ball that is rolling and slipping is more appropriately described by kinetic friction, which is typically smaller than the maximum static friction. A difference of about 5% between kinetic and static friction coefficients was measured in Ref. 5 for materials similar to the ones used in this work. This difference is of the order of the uncertainty we have in the measurement of μ carried out in this work.

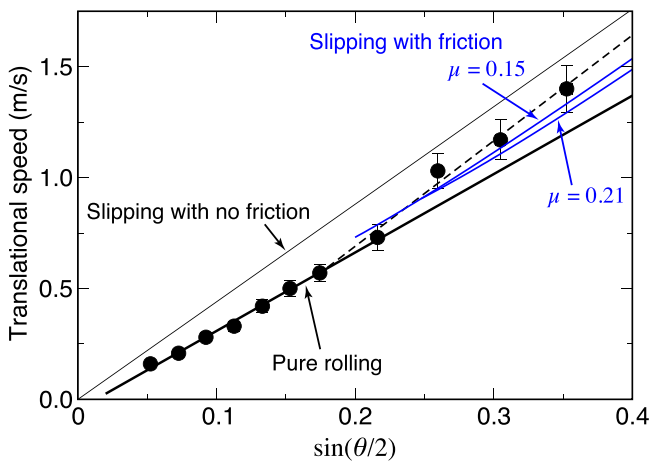

Fig. 8. Behavior of the translational ball speed ($R\dot{\theta}$) as function of $\sin(\theta/2)$ during the motion on the track. The thick line corresponds to a linear fit for $\sin(\theta/2) < 0.2$, and corresponds to pure rolling (coefficient of determination 0.9978). The gray lines (blue online) correspond to Eq. (7) for different friction coefficients (these curves start at $\sin(\theta_s/2)$ for the respective μ). The thin line corresponds to Eq. (7) with $\mu = 0$ and $\theta_s = 0$ (slipping with no friction). The dashed line is a guide to the eye. The error bars for $\sin(\theta/2)$ are smaller than the size of the points.

Finally, we note a couple of minor changes that could improve the apparatus. A larger track radius will increase the values of all relevant times (e.g., t_f and t_c) and this should reduce the relative uncertainties on those quantities. In addition, we expect that a larger ball will improve both voltage and sound signals. The use of video analysis[11,12] would also help to identify and to visualize the transition between rolling and slipping. And finally, the cost of the apparatus could be reduced by replacing the aluminum track with a wooden track covered by a thin metallic plate.

VI. CONCLUSIONS

We have constructed an apparatus to determine the angle a ball loses contact with a circular track, and to study how the ball moves when it is on the track. The apparatus was constructed based on a textbook problem and it can be used in classrooms to illustrate the concepts of friction, rolling, and slipping, as well as to encourage discussions about the phenomena (e.g., the rolling-to-slipping transition) that appear in real situations.

ACKNOWLEDGMENTS

The authors thank Rodrigo L. Ximenez and João F. Viana for helping us with the photodetector setup and with the electrical conductivity of the circular track. The authors also thank Cesar D. Bazana from Pro-metal Industrial Ltda for building the aluminum rails and Professor Ivan de Oliveira for helpful discussions. D.C.S. acknowledges the scholarship from the SAE/UNICAMP. The financial support from UNICAMP is also acknowledged.

[a]Electronic mail: vitor@ft.unicamp.br

[1]H. D. Young, R. A. Freedman, and A. L. Ford, *Sears and Zemansky's University Physics with Modern Physics*, 12nd ed. (Addison-Wesley, San Francisco, 2008), p. 244.
[2]M. Alonso and E. J. Finn, *Fundamental University* Physics, 1st ed. (Addison-Wesley Publication Co, Reading, MA, 1967), Vol. 1.
[3]J. Walker, D. Halliday, and R. Resnick, *Fundamentals of Physics*, 10th ed. (John Wiley & Sons Inc., Hoboken, NJ, 2013), Vol. 1, p. 205 ex. 34.
[4]K. R. Symon, *Mechanics*, 2nd ed. (Addison-Wesley, Reading, MA, 1961), p. 376.
[5]D. E. Shaw and F. J. Wunderlich, "Study of the slipping of a rolling sphere," Am. J. Phys. **52**, 997–1000 (1984).
[6]R. L. Chaplin and M. G. Miller, "Coefficient of friction for a sphere," Am. J. Phys. **52**, 1108–1111 (1984).
[7]A. Doménech, T. Doménech, and J. Cebrián, "Introduction to the study of rolling friction," Am. J. Phys. **55**, 231–235 (1987).
[8]Q. Song, "The requirement of a sphere rolling without slipping down a grooved track for the coefficient of static friction," Am. J. Phys. **56**, 1145–1146 (1988).
[9]F. S. Crawford, "Rolling and slipping down Galileo's inclined plane: Rhythms of the spheres," Am. J. Phys. **64**, 541–546 (1996).

[10]M. Basta, M. Di Gennaro, and V. Picciarelli, "A desktop apparatus for studying rolling motion," Phys. Educ. **34**, 371–375 (1999).
[11]S. Phommarach, P. Wattanakasiwich, and I. Johnston, "Video analysis of rolling cylinders," Phys. Educ. **47**, 189–196 (2012).
[12]Anna De Ambrosis, M. Malgieri, P. Mascheretti, and P. Onorato, "Investigating the role of sliding friction in rolling motion: A teaching sequence based on experiments and simulations," Eur. J. Phys. **36**, 035020 (2015).
[13]The Rayleigh's dissipation function is used to derive the expressions of dissipative forces that can not be obtained from a potential energy function. These expressions are then used in the Lagrange's equations in a formulation that accommodates dissipation.
[14]H. Goldstein, C. Poole, and J. Safko, *Classical Mechanics*, 3rd ed. (Addison-Wesley, Reading, MA, 2000), pp. 22–24.
[15]Details of the sound sensor can be determined at <http://www.dfrobot.com/wiki/index.php/Analog_Sound_Sensor_SKU:_DFR0034>.
[16]Details of the SD module can be determined at <http://www.dfrobot.com/wiki/index.php/SD_Module_(SKU:_DFR0071)>.
[17]See supplementary material at http://dx.doi.org/10.1119/1.4972177 for circuit diagrams and Arduino code.

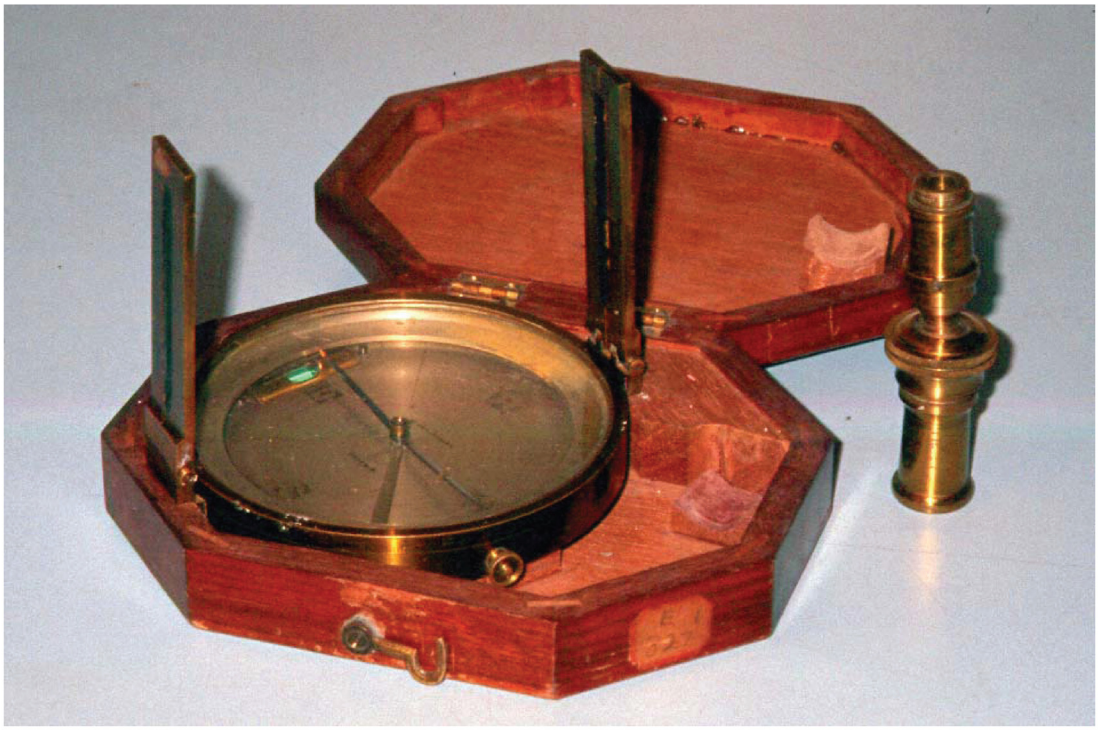

Surveyor's Compass

The standard undergraduate curriculum in the second half of the 19th century often included a required course in surveying and land measurement. Thus I was prepared to find this surveyor's compass at the physics department at the flagship campus of the University of Texas in Austin, which was founded in 1883. It was made by Gurley of Troy New York, the largest maker of surveying equipment in the United States at the time. (Picture and Notes by Thomas B. Greenslade, Jr., Kenyon College)